

A Cell-Free Scheme for UAV Base Stations with HAPS-Assisted Backhauling in Terahertz Band

Omid Abbasi

Halim Yanikomeroglu

Abstract—In this paper, we propose a cell-free scheme for unmanned-aerial-vehicle (UAV) base-stations (BSs) to manage the severe intercell interference between aerial and terrestrial nodes. Since the cell-free scheme requires a huge bandwidth for backhauling, we propose to use the terahertz (THz) band for the wireless backhaul links between UAV-BSs and central-processing-unit (CPU). Also, because the THz band requires a reliable line-of-sight (LoS) link, instead of a terrestrial CPU, we propose to use a high-altitude-platform-station (HAPS) as a CPU. At the first time-slot of the proposed scheme, users send their messages to UAVs at the sub-6 GHz band. Then each UAV applies match-filtering to align the received signals from users, and performs power allocation for the aligned signal of each user. At the second time-slot, we allocate orthogonal resource-blocks (RBs) for each user at the THz band, and send signals towards HAPS. In HAPS, for aligning the received signals for each user from different UAVs, we perform analog beamforming. Finally, we demodulate and decode the message of each user at its unique RBs. We formulate an optimization problem that maximizes the minimum SINR of users, and find the optimum allocated powers for users in each UAV by the bisection method. Simulation results prove the superiority of the proposed scheme compared with aerial-cellular and terrestrial-cell-free baseline schemes. Simulation results also showed that utilizing HAPS as a CPU is useful when the huge path-loss between UAV-BSs and HAPS in the THz band is compensated by a high number of antennas at HAPS.

Index Terms—UAV BS, cell-free, HAPS, THz, backhaul.

I. INTRODUCTION AND MOTIVATION

The application of Unmanned aerial vehicles (UAVs) as a base station (BS), that is called UxNB [1], has attracted substantial attention for 5G and beyond-5G due to their many advantages such as high mobility, on-demand deployment, and a high probability of establishing a line of sight (LoS) link with users [2]. However, the severe intercell interference in aerial networks, which is due to the possible LoS link among users and UxNBs at neighbor cells, is a big problem.

Cell-free massive multiple input multiple output (MIMO) is another technology that has been proposed for beyond 5G [3]. In this technology, each user is served by a massive number of access points (APs), and all of these APs are connected to a central processing unit (CPU) [4]. Indeed, in this method, the interference from other cells is utilized as the desired signal, and all of these received signals of APs are combined at the CPU. In our work, we propose to apply this cell-free

scheme for a set of aerial APs (UxNBs) to manage the severe interference in aerial networks between aerial and terrestrial nodes. There are many works in the literature that investigate cell-free scheme for terrestrial networks [3], [4]. However, to the best of our knowledge, our work is the first one that considers the cell-free scheme for UAV BSs.

In the cell-free scheme, a huge bandwidth is required for backhaul links between UxNBs and CPU. For terrestrial cell-free APs, this huge bandwidth for backhauling can be provided by fiber links [4]. However, for the proposed aerial cell-free APs, this backhauling must be both wireless and at the upper frequency bands. The problem is that due to dynamic blockages and shadowing between UxNBs and a terrestrial CPU, it is hard to utilize the upper frequency bands (e.g., the terahertz (THz) band) for these wireless backhaul links between UxNBs and terrestrial CPU [5]. Indeed, higher frequency bands require a reliable LoS link, and probabilistic LoS links between UAVs and terrestrial CPU is not suitable for these bands.

The application of High altitude platform station (HAPS) in wireless networks has attracted a lot of attention recently [6]. HAPS is deployed in the stratosphere and has a fixed position related to the earth. In this work, instead of a terrestrial CPU, we propose to utilize HAPS as an aerial CPU to combine all the received signals from all UxNBs¹. HAPS is a perfect choice to work as a CPU for our proposed cell-free scheme since there is negligible blockage and shadowing between HAPS and UxNBs which leads to a reliable LoS link. Hence, we can easily use the upper frequency bands for these links to support the huge bandwidth requirement for backhauling of the proposed cell-free scheme. We propose to use the THz frequency band for these backhaul links. The THz band is generally defined as the region of the electromagnetic spectrum in the range of 100 GHz to 10 THz. The D band (110 – 170 GHz) is among the next interesting range of frequencies for beyond-5G systems [8], and hence we consider this band as the carrier frequency at this work.

II. SYSTEM MODEL AND CHANNEL MODEL

A. System Model

We can see the proposed cell-free scheme with HAPS-assisted THz backhauling in Fig. 1. We see that M UxNBs

This work was supported by Huawei Canada Co., Ltd.

O. Abbasi and H. Yanikomeroglu are with the Department of Systems and Computer Engineering, Carleton University, Ottawa, ON K1S5B6, Canada. e-mail: omidabbasi@sce.carleton.ca; halim@sce.carleton.ca

¹Note that HAPS is generally deployed for many other applications such as super-macro-base-station, computing, sensing, and localization. In this paper, we propose to utilize it as a CPU node for backhauling as well [6], [7].

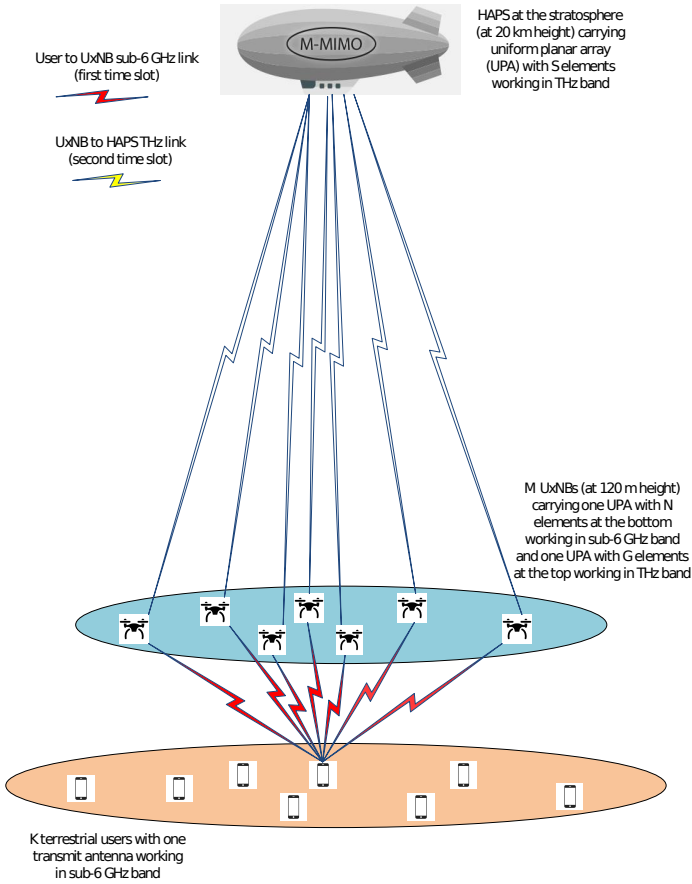


Fig. 1: System model for the proposed cell-free scheme with HAPS-assisted THz backhauling.

are serving K users in the cell-free mode. Each UxNB is assumed to be equipped with a uniform planar array (UPA) with N receive antenna elements under the drone's bottom working in sub-6 GHz frequency band, and a UPA with G transmit antenna elements on top of the drone working in the THz band. We propose to utilize a HAPS as a CPU to combine the received signals of all UxNBs and decode the messages of all K users. HAPS is equipped with a UPA with S receive antenna elements working in the THz band.

In the proposed scheme, the transmission is performed in two time slots. At the first time slot, users send their data to UxNBs. At each UxNB, the channel state information (CSI) of user-to-UxNB links are estimated and then are utilized for match filtering of received signals. We also allocate the total power of each UxNB among the users. At the second time slot, UxNBs forward the power-allocated and match-filtered signals towards HAPS. Note that we utilize the THz band for UxNB to HAPS link, and we allocate orthogonal resource blocks (RBs) for each user's signal at these backhaul links. This means that we need K times more bandwidth for backhauling which can be satisfied in the THz band. In order to align the received signals for each user from different UxNBs, we perform analog beamforming based on the steering vectors of the UPA at HAPS for all UxNBs. Finally, we demodulate and decode the

message of each user at its own unique RBs.

B. Channel Model

In this paper, the channel between user k and antenna n of UxNB m is indicated by h_{kmn} which includes both large scale fading, i.e., path loss and shadowing, and multipath small scale fading effects. Note that we assume a UPA for the receiver of UAV with $N = N_w \times N_l$ antenna elements in which N_w and N_l show the number of antenna elements in the width and length of array, respectively. Because there exist a LoS link between users and drones, a Ricean distribution is considered for the channel between user k and antenna $n = (n_w, n_l)$ of UxNB m as $h_{kmn} = \frac{PL_{km}}{10^{-20}} (\sqrt{P_{km}^{LoS}} a_{kmn} + \sqrt{P_{km}^{NLoS}} CN(0, 1))$, in which $CN(0, 1)$ shows a complex normal random variable with the mean value of 0 and the variance (power) of 1. $a_{kmn} = \exp(j2\pi(\frac{d_{km}}{\lambda_{sub6}})) \times \exp(j2\pi(\frac{d_{sub6,w}(n_w-1) \sin \theta_{km} \cos \phi_{km}}{\lambda_{sub6}})) \times \exp(j2\pi(\frac{d_{sub6,l}(n_l-1) \sin \theta_{km} \sin \phi_{km}}{\lambda_{sub6}}))$ indicates the phase shift of the LoS link signal due to distance in which d_{km} shows the distance between user k and UxNB m , $d_{sub6,w} = \frac{\lambda_{sub6}}{2}$ ($d_{sub6,l} = \frac{\lambda_{sub6}}{2}$) is the element spacing at the width (length) of antenna array for each UxNB in sub-6 GHz frequency band f_{sub6} , $\lambda_{sub6} = \frac{C}{f_{sub6}}$ is the wavelength, and $C = 3 \times 10^8$ m/s is the light speed. θ_{km} and ϕ_{km} show the elevation and azimuth angle of arrivals of the transmitted signal from user k at the reference antenna element of UxNB m . Note that $\mathbf{a}_{km} = [a_{kmn}]_{1 \times N}$ creates the steering vector of the receive antenna array of UAV m for user k . Also, we have $PL_{km} = P_{km}^{LoS} PL_{km}^{LoS} + P_{km}^{NLoS} PL_{km}^{NLoS}$ in which according to [9], for the LoS and non-LoS (NLoS) path loss of UxNB m and user k link we can write $PL_{km}^{LoS} = FSPL_{km} + \eta_{LoS}^{dB}$, and $PL_{km}^{NLoS} = FSPL_{km} + \eta_{LoS}^{dB}$, respectively. In these equations, $FSPL_{km} = 10 \log(\frac{4\pi f_{sub6} d_{km}}{C})^2$ shows the free space pathloss (FSPL), and η_{LoS}^{dB} and η_{NLoS}^{dB} indicate the excessive path losses (in dB) affecting the air to ground links at LoS and NLoS cases, respectively. P_{km}^{LoS} shows the probability of establishing LoS link between user k and UxNB m [9] as $P_{km}^{LoS} = \frac{1}{1 + A \exp(-B(90 - \theta_{km}) - A)}$, in which θ_{km} (in degree) shows the elevation angle between user k and UxNB m , and A and B are parameters depending on the environment. $P_{km}^{NLoS} = 1 - P_{km}^{LoS}$ shows the probability of establishing NLoS link between user k and UxNB m .

The large scale channel power gain for the user k to UxNB m link is equal to $\beta_{km}^2 = E\{|h_{kmn}|^2\} = E\{h_{kmn} h_{kmn}^*\} = 10^{-\frac{PL_{km}}{10}} = 10^{-\frac{P_{km}^{LoS} PL_{km}^{LoS} + P_{km}^{NLoS} PL_{km}^{NLoS}}{10}}$. By considering $\beta_0 = (\frac{4\pi f_{sub6}}{C})^{-2}$ as the channel gain at the reference distance $d_{km} = 1$ m, the large scale channel power gain can be rewritten as $\beta_{km}^2 = \eta_{km} \beta_0 (d_{km})^{-2}$, in which $\eta_{km} = 10^{-\frac{P_{km}^{LoS} \eta_{LoS}^{dB} + P_{km}^{NLoS} \eta_{NLoS}^{dB}}{10}}$ shows the excessive pathloss. We consider independent additive white Gaussian noise (AWGN) with the distribution $CN(0, \sigma_m^2)$ at antenna n of UxNB m .

We assume a UPA for the transmitter of each UxNB with $G = G_w \times G_l$ antenna elements in which G_w and G_l show the number of antenna elements in the width and length of

array, respectively. We also assume a UPA at the receiver of HAPS with a large number of $S = S_w \times S_l$ antenna elements in which S_w and S_l show the number of antenna elements in the width and length of array, respectively. The channel between transmit antenna $g = (g_w, g_l)$ of UxNB m and receiver antenna $s = (s_w, s_l)$ of HAPS is assumed to be LoS, and is equal to $g_{mgs} = \gamma_m b_{mg}^* c_{ms}$ in which $b_{mg} = \exp(j2\pi(\frac{d_m}{\lambda_{\text{THz}}})) \exp(j2\pi(\frac{d_{\text{THz,d,w}}(g_w-1) \sin \Theta_m \cos \Phi_m}{\lambda_{\text{THz}}})) \times \exp(j2\pi(\frac{d_{\text{THz,d,l}}(g_l-1) \sin \Theta_m \sin \Phi_m}{\lambda_{\text{THz}}}))$ indicates the phase shift of the transmitted signal at transmitter. Also, $c_{ms} = \exp(j2\pi(\frac{d_{\text{THz,h,w}}(s_w-1) \sin \Theta_m \cos \Phi_m}{\lambda_{\text{THz}}})) \times \exp(j2\pi(\frac{d_{\text{THz,h,l}}(s_l-1) \sin \Theta_m \sin \Phi_m}{\lambda_{\text{THz}}}))$ indicates the phase shift of the transmitted signal at and receiver. In these equations, d_m indicate the distance between the reference antenna element of UxNB m and the reference antenna element of HAPS, $d_{\text{THz,d,w}} = \frac{\lambda_{\text{THz}}}{2} (d_{\text{THz,d,l}} = \frac{\lambda_{\text{THz}}}{2})$ is the element spacing at the width (length) of transmit antenna array at each UxNB in THz frequency band f_{THz} , $d_{\text{THz,h,w}} = \frac{\lambda_{\text{THz}}}{2} (d_{\text{THz,h,l}} = \frac{\lambda_{\text{THz}}}{2})$ is the element spacing at the width (length) of receiver antenna array at HAPS in THz frequency band f_{THz} , and $\lambda_{\text{THz}} = \frac{c}{f_{\text{THz}}}$ is the wavelength. Also, Θ_m and Φ_m show the elevation and azimuth angles of the transmitted signal from UxNB m at the reference antenna element of HAPS. Note that $\mathbf{b}_m = [b_{mg}]_{1 \times G}$ creates the steering vector of the transmit antenna array of UAV m , and $\mathbf{c}_m = [c_{ms}]_{1 \times S}$ creates the steering vector of the receive antenna array of HAPS for each UxNB m . γ_m^2 shows the path loss between UxNB m and HAPS. The path loss for THz band is given by $\gamma_m^2 = \gamma_0 d_m^{-2} \tau_m$ in which $\gamma_0 = (\frac{4\pi f_{\text{THz}}}{c})^{-2}$ is the channel gain at the reference distance $d_m = 1$ m [10]. $\tau_m = e^{-K d_m}$ shows the transmittance of the medium in which K (in dB/km) is the absorption coefficient of THz medium that is a function of frequency and altitude. We consider independent AWGN with the distribution $CN(0, \sigma_H^2)$ at HAPS.

III. PROPOSED TRANSCEIVER SCHEMES

We can see the proposed transceiver scheme at UxNB m in Fig. 2. At the first slot of the proposed scheme, each user transmits its message to the UxNBs. The transmitted signal by user k is shown by $\sqrt{P_k} s_k$ in which P_k (for $k \in \{1, 2, \dots, K\}$) indicate the maximum transmit power at each user k , and s_k ($E\{|s_k|^2\} = 1$) is the transmitted symbol from user k . The received signal at the antenna n of UxNB m 's UPA equals $y_{mn} = \sum_{k=1}^K h_{kmn} \sqrt{P_k} s_k + z_m$ in which z_m is the AWGN noise at the UxNB m . After receiving y_{mn} at the antenna n of UxNB m , at the digital baseband beamforming block for each user, according to the estimated CSI for the channel between user k and antenna n of UxNB m , i.e., h_{kmn} , we perform match filtering as $y_{kmn}^{\text{MF}} = y_{mn} \times \frac{h_{kmn}^*}{|h_{kmn}|}$, and combine these match-filtered signals to have $y_{km}^{\text{COMB}} = \sum_{n=1}^N y_{kmn}^{\text{MF}}$. Note that x^* indicates the conjugate of x . Then, we allocate the power P_{km} for each user so that we must have $\sum_{k=1}^K P_{km} \leq P_m$ for each UxNB m , in which P_m shows the total power at UxNB m . Note that we need to normalize the signal for each user before power allocation as $y_{km}^{\text{NORM}} = \frac{y_{km}^{\text{COMB}}}{|y_{km}^{\text{COMB}}|}$ in which $|x|$

shows the absolute value of x . Therefore, the signal for each user after power normalization and power allocation will be $y_{km} = \sqrt{P_{km}} y_{km}^{\text{NORM}}$. In order to transmit these K signals to the HAPS, we allocate orthogonal frequency RBs for each of them to avoid interference and then combine them. Finally, we perform analog beamforming with phase shifter (PSs) to direct the transmitted signal from each UxNB towards HAPS. This is done by multiplying the signal by b_{mg}^* at each transmit antenna g of each UxNB m . Note that the transmitted signal for user k from antenna g of UxNB m equals $b_{mg} y_{km}$.

The transmitted signal from each UxNB will be received at each antenna s of HAPS after passing through the UxNB m to antenna s of HAPS channel, i.e., g_{mps} . Hence, the received signal in the RB k and at the antenna s of HAPS will be $y_s^k = \sum_{m=1}^M \sum_{g=1}^G g_{mps} b_{mg} y_{km} + z_H = \sum_{m=1}^M \sum_{g=1}^G c_{ms} \gamma_m b_{mg} b_{mg}^* y_{km} + z_H = \sum_{m=1}^M \sum_{g=1}^G c_{ms} \gamma_m y_{km} + z_H$, in which z_H is the AWGN noise at each receive antenna of HAPS. Superscript k shows the received signal at RB k . In the proposed receiver scheme at HAPS, we perform analog beamforming with PSs to align the received signals from each UxNB m at the receive antennas of HAPS. For this end, we multiply the signal y_s^k by c_{ms}^* for all UxNBs and HAPS receive antennas, and then combine these signals as $y^k = \sum_{m=1}^M \sum_{s=1}^S c_{ms}^* y_s^k$. As we mentioned, because we allocate orthogonal RBs for each user at the UxNB to HAPS THz links, the received signal for each user can be separately achieved at the HAPS. Finally, utilizing this signal y^k , we demodulate and decode the symbol of each user k .

Now, we derive the SINR of each user utilizing the signal y^k . After some manipulation, this signal can be written as in (1) at the top of next page. From (1), by defining $F_{\text{NORM}} = \frac{\sqrt{N}}{M} \sqrt{\sum_{m=1}^M \sum_{k'=1}^K \beta_{k'm}^2 P_{k'} + M \sigma^2}$, and after some manipulations, the expectation of the desired signal for user k can be written as $E[\text{DS}_k] = \frac{GNS\sqrt{P_k}}{F_{\text{NORM}}} \sum_{m=1}^M \gamma_m \sqrt{P_{km}} \beta_{km}$. Next, we derive the variance of the interference terms in (1) for user k in which we can see there are two types of interference. The first type is due to the interference from other users, and we show it with $I_{k,U}$, and the second type is due to the amplified noise at UxNBs, and we indicate it with $I_{k,N}$. For $I_{k,U}$, after some manipulations, we can write $E[I_{k,U} \times I_{k,U}^*] = \frac{N S G^2}{F_{\text{NORM}}^2} \sum_{m=1}^M \gamma_m^2 P_{km} \sum_{k'=1}^K \beta_{k'm}^2 P_{k'}$, and for $I_{k,N}$ we have $E[I_{k,N} I_{k,N}^*] = \frac{N S G^2}{F_{\text{NORM}}^2} \sum_{m=1}^M \gamma_m^2 P_{km} \sigma^2$. Finally, we show the noise term at HAPS with N_{HAPS} which has a variance equal to $E[N_{\text{HAPS}} N_{\text{HAPS}}^*] = M S \sigma_H^2$. Now, according to derived formulas for $E[\text{DS}_k]$, $E[I_{k,U} \times I_{k,U}^*]$, $E[I_{k,N} \times I_{k,N}^*]$, and $E[N_{\text{HAPS}} N_{\text{HAPS}}^*]$, we derive the SINR of the user k with the proposed scheme in (2) at the top of the next page. Utilizing this SINR, we can derive the achievable rate of user k as $R_k = \log_2(1 + \text{SINR}_k)$.

IV. OPTIMIZATION PROBLEM

In this section, we formulate an optimization problem that maximizes the minimum SINR of users by finding the

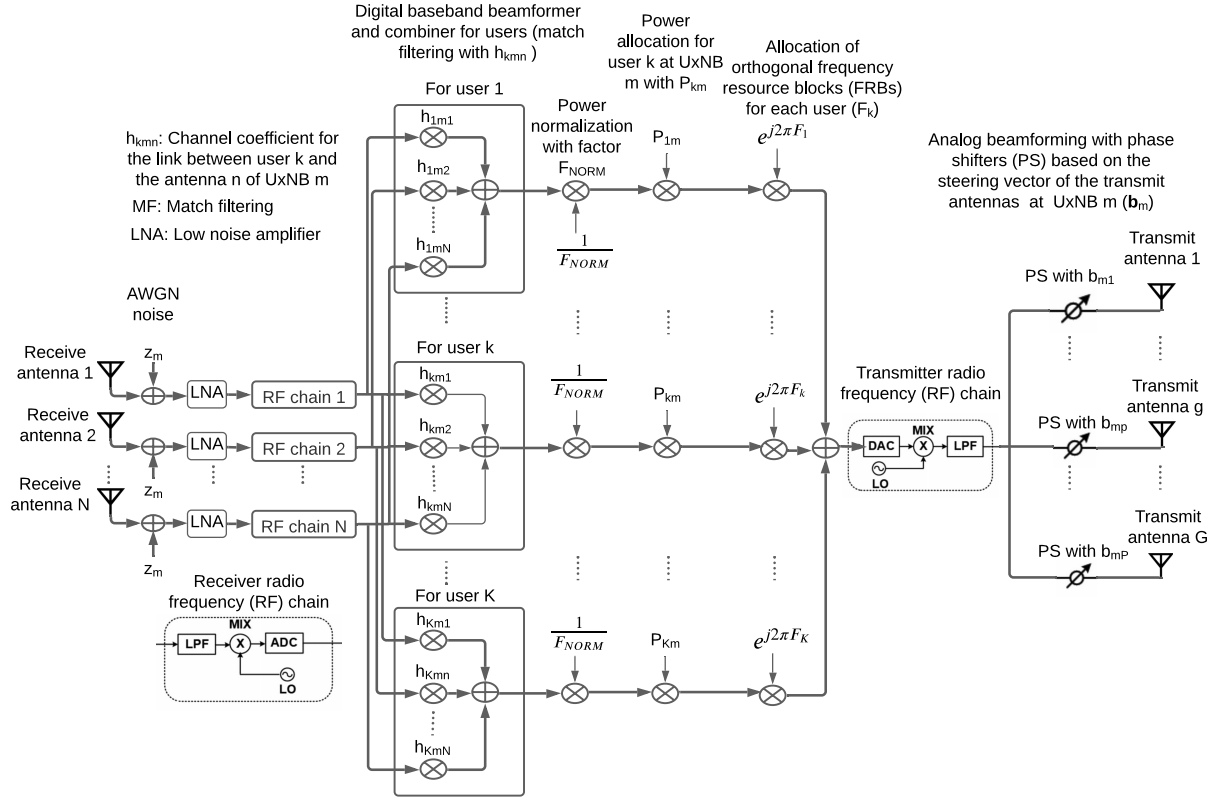


Fig. 2: The proposed transceiver scheme at UxNB m .

$$y^k = \sum_{m=1}^M \sum_{s=1}^S c_{ms}^* y_s^k = \sum_{m=1}^M \sum_{s=1}^S c_{ms}^* (G \sum_{m'=1}^M c_{m's} \gamma_{m'} \sqrt{P_{km'}} \frac{\sum_{n=1}^N (\sum_{k'=1}^K h_{k'm'n} \sqrt{P_{k'}} s_{k'} + z_{m'}) \times \frac{h_{km'n}^*}{|h_{km'n}|}}{|\sum_{n=1}^N (\sum_{k'=1}^K h_{k'm'n} \sqrt{P_{k'}} s_{k'} + z_{m'}) \times \frac{h_{km'n}^*}{|h_{km'n}|}|} + z_H). \quad (1)$$

$$\text{SINR}_k = \frac{E[\text{DS}_k]^2}{E[I_{k,U} I_{k,U}^*] + E[I_{k,N} I_{k,N}^*] + E[N_{\text{HAPS}} N_{\text{HAPS}}^*]} \quad (2)$$

$$= \frac{MG^2 N S P_k (\sum_{m=1}^M \gamma_m \sqrt{P_{km}} \beta_{km})^2}{MG^2 \sum_{m=1}^M \gamma_m^2 P_{km} \sum_{k'=1}^K \beta_{k'm}^2 P_{k'} + MG^2 \sum_{m=1}^M \gamma_m^2 P_{km} \sigma^2 + \sigma_H^2 (\sum_{m=1}^M \sum_{k'=1}^K \beta_{k'm}^2 P_{k'} + M \sigma^2)}. \quad (3)$$

optimum allocated powers for users in each UxNB, i.e., $\mathbf{P} = [P_{km}]_{K \times M}$. We can write the optimization problem as

$$(P): \max_{\mathbf{P}} \min_k \text{SINR}_k \quad (4)$$

$$\text{s.t.} \quad \sum_{k=1}^K P_{km} \leq P_m, \quad \forall m, \quad (5)$$

$$P_{km} > 0, \quad \forall k, \forall m, \quad (6)$$

efficiently by the bisection method [11]. For this end, we rewrite the problem (P) as

$$(P1): \max_{\mathbf{P}, \eta} \eta \quad (7)$$

$$\text{s.t.} \quad \text{SINR}_k \geq \eta, \quad \forall k \quad (8)$$

$$\sum_{k=1}^K P_{km} \leq P_m, \quad \forall m, \quad (9)$$

$$P_{km} > 0, \quad \forall k, \forall m. \quad (10)$$

where constraint (5) shows the maximum total power constraint at each UxNB m . Problem (P) is a quasi-concave optimization problem and its optimal solution can be found

It can be easily proved that (P1) is equivalent to (P). By performing the variable change $\mathbf{T} = [P_{km}^2]_{K \times M}$, for any given value of η , problem (P1) will be a convex feasibility problem that can be solved optimally by convex optimization

techniques such as the interior-point method. The summary of this bisection method is shown in Algorithm 1.

Algorithm 1 Bisection method for solving power allocation problem (P).

- 1: Initialize the values of η_{\min} and η_{\max} , where η_{\min} and η_{\max} show a range for the minimum SINR of users. Choose a tolerance $\epsilon > 0$.
- 2: **repeat**
- 3: Set $\eta = \frac{\eta_{\min} + \eta_{\max}}{2}$, and solve the convex feasibility problem (P1) by the interior-point method.
- 4: If the problem (P1) is feasible, set $\eta_{\min} = \eta$, else set $\eta_{\max} = \eta$.
- 5: **until** $\eta_{\max} - \eta_{\min} < \epsilon$.

V. NUMERICAL RESULTS

In this section, numerical results are provided in order to show the performance gain of the proposed scheme. The following default parameters are applied in the simulations except that we specify different values for them. For the carrier frequency of first and second hops, we assume $f_{\text{sub6}} = 2$ GHz and $f_{\text{THz}} = 120$ GHz, respectively. The communication bandwidth is assumed to be $BW = 1$ MHz, and the noise power spectral density is equal to $N_0 = -174$ dBm/Hz. We assume that all users are uniformly distributed in a square with a length of 1000 meters. Also, we assume that the maximum transmit power at each user and each UxNB equal $P_k = 0.2$ W, $\forall k$ and $P_m = 25$ dBm, $\forall m$, respectively. Considering an urban area, the excessive path losses affecting the air to ground links at LoS and NLoS cases are assumed $\eta_{\text{LoS}}^{\text{dB}} = 1$ dB and $\eta_{\text{NLoS}}^{\text{dB}} = 20$ dB, respectively. Also, for the urban area, we have $A = 9.61$ and $B = 0.16$. The absorption coefficient of THz medium is equal to $K = 0.5$ dB/km. We assume a uniform square placement for M UAVs, and a fixed flight height $h = 120$ m for all of the UAVs. In Algorithm 1, we set initial values as $\eta_{\min} = 0$ and $\eta_{\max} = 1500$, and also the tolerance value as $\epsilon = 0.01$. We also consider the HAPS altitude as 20 km.

In the simulation figures, we compared the proposed scheme, which is called **aerial cell-free scheme**, with two baseline schemes. **1) Aerial cellular scheme** in which each terrestrial user is served by only one UxNBs. At this baseline method, all of the other parameters and channel models are the same as the proposed scheme. **2) Terrestrial cell-free scheme** in which each terrestrial user is served by many terrestrial access points, and a perfect backhaul with fiber links is considered between access points and CPU. At this baseline scheme, the Rayleigh fading model is considered for the channels between users and APs. Also, in order to have a fair comparison, the number of receive antennas at terrestrial APs is assumed to be the same as the number of receive antennas at UxNBs (N) in aerial schemes.

Fig. 3 shows the achievable minimum rate per user versus the total power of each UxNB. We can see that the proposed aerial cell-free scheme has a better performance

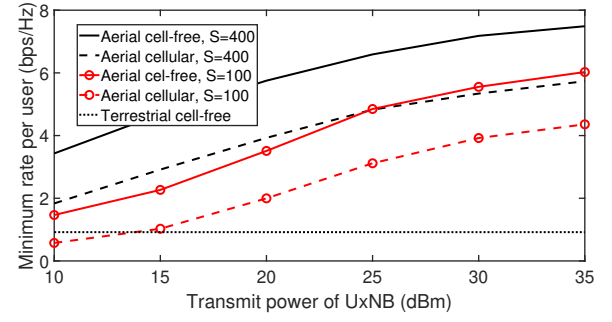


Fig. 3: The achievable minimum rate per user versus total power of each UxNB ($P_1 = \dots = P_M$) for the aerial and terrestrial BSs with cell-free and cellular schemes. We set $K = 16$, $M = 16$, $N = 4$, and $G = 9$.

compared with the aerial cellular scheme for both values of S . Indeed, due to the severe intercell interference from other users at neighbor cells in the aerial cellular scheme, our proposed scheme has much better performance than this baseline scheme. In this figure, we can also see the terrestrial cell-free baseline scheme that is not a function of its access points power as we considered a perfect backhaul for this scheme. Our proposed scheme has much better performance than this baseline scheme as well. This is because in the terrestrial cell-free scheme, due to a high path loss and shadowing, the link between a user and far access points can be very weak, and hence working in cell-free mode is not useful. However, in the proposed aerial cell-free scheme, since there is a strong LoS link between users and UxNBs, the signal of each user is received at many UxNBs, and hence cell-free scheme is useful for the proposed system model.

Fig. 4 shows the achievable minimum rate per user versus the number of UxNBs (M) for the aerial and terrestrial BSs with cell-free and cellular schemes. We can see that the proposed aerial cell-free scheme outperforms the aerial cellular scheme for both values of S . It is shown that by increasing M , the improvement in the performance of aerial schemes is much more than the terrestrial scheme which is because of a higher probability of establishing LoS links between UxNBs and users for a larger M in aerial schemes. One can also see that the superiority of aerial cell-free scheme over aerial cellular scheme increases by M which is due to a higher intercell interference for the cellular scheme at a higher M .

Fig. 5 indicates the achievable minimum rate per user versus the number of HAPS antennas (S). One can see that when the number of HAPS antennas is small, the performance of aerial and terrestrial schemes are close. For example when $S = 16$, the terrestrial cell-free scheme has better performance rather than the aerial cellular scheme and it has a close performance compared with the proposed aerial cell-free scheme. However, when the number of HAPS antennas is big, both aerial schemes have significant performance gain over the terrestrial cell-free scheme. This figure shows that utilizing HAPS as a CPU is useful when the huge path loss between UxNBs and

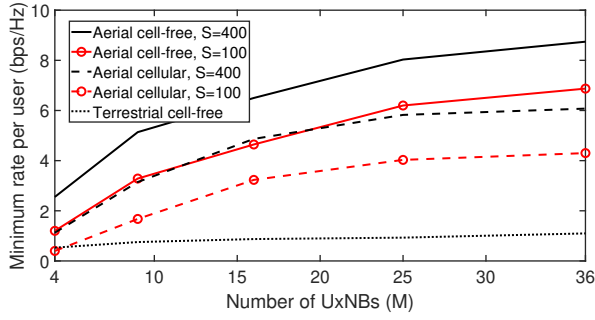


Fig. 4: The achievable minimum rate per user versus the number of UxNBs (M) for the aerial and terrestrial BSs with cell-free and cellular schemes. We set $P_m = 25$ dBm, $\forall m$, $K = 16$, $N = 4$, and $G = 9$.

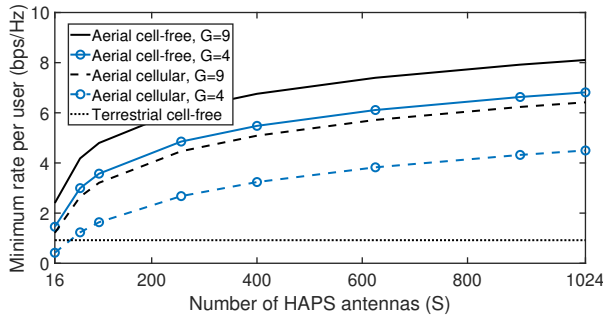


Fig. 5: The achievable minimum rate per user versus number of HAPS antennas (S) for the aerial and terrestrial BSs with cell-free and cellular schemes. We set $P_m = 25$ dBm, $\forall m$, $M = 16$, $K = 16$, $N = 4$, and $G = 4, 9$.

HAPS in the THz band is compensated by a high number of antennas at HAPS.

Fig. 6 shows the CDF of the minimum rate per user. We can see that the proposed aerial cell-free scheme has a better performance compared with both aerial cellular and terrestrial cell-free baseline schemes for both values of M . We can also see that the aerial cellular scheme outperforms the terrestrial cell-free scheme which is because of establishing LoS links between users and UxNBs in the aerial networks. From this figure, we can see that the variance of the minimum achievable rate per user for the cell-free scheme is less than the cellular one. Also, one can see that increasing the number of UxNBs reduces the variance of the minimum achievable rate per user for both aerial cell-free and aerial cellular schemes.

VI. CONCLUSION

In this paper, we proposed a cell-free scheme for a set of UxNBs to manage the severe interference in aerial networks between aerial and terrestrial nodes. We also proposed to use a HAPS as a CPU to combine all the received signals from all UxNBs in the THz band. Next, we proposed a transceiver scheme at UxNBs and a receiver scheme at HAPS, and formulated an optimization problem to maximize the minimum

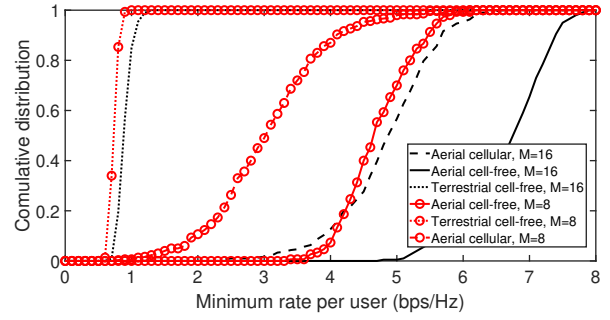


Fig. 6: The CDF of the minimum rate per user ($R_1 = \dots = R_K$) for the aerial and terrestrial BSs with cell-free and cellular schemes. We set $P_m = 25$ dBm, $\forall m$, $K = 16$, $S = 400$, $N = 4$, and $G = 9$.

SINR of users. Simulation results proved the superiority of the proposed scheme compared with aerial cellular and terrestrial cell-free baseline schemes which is due to the existence of LoS links between users and UxNBs. Simulation results also showed that utilizing HAPS as a CPU is useful when the huge path loss between UxNBs and HAPS in the THz band is compensated by a high number of antennas at HAPS.

REFERENCES

- [1] O. Abbasi, H. Yanikomeroglu, A. Ebrahimi, and N. M. Yamchi, "Trajectory design and power allocation for drone-assisted NR-V2X network with dynamic NOMA/OMA," *IEEE Transactions on Wireless Communications*, vol. 19, no. 11, pp. 7153–7168, Nov. 2020.
- [2] E. Kalantari, H. Yanikomeroglu, and A. Yongacoglu, "On the number and 3D placement of drone base stations in wireless cellular networks," in *2016 IEEE 84th Vehicular Technology Conference (VTC-Fall)*, pp. 1–6.
- [3] E. Nayebe, A. Ashikhmin, T. L. Marzetta, H. Yang, and B. D. Rao, "Precoding and power optimization in cell-free massive MIMO systems," *IEEE Transactions on Wireless Communications*, vol. 16, no. 7, pp. 4445–4459, Jul. 2017.
- [4] H. Q. Ngo, A. Ashikhmin, H. Yang, E. G. Larsson, and T. L. Marzetta, "Cell-free massive MIMO versus small cells," *IEEE Transactions on Wireless Communications*, vol. 16, no. 3, pp. 1834–1850, Mar. 2017.
- [5] M. Gapeyenko, V. Petrov, D. Moltchanov, S. Andreev, N. Himayat, and Y. Koucheryavy, "Flexible and reliable UAV-assisted backhaul operation in 5G mmwave cellular networks," *IEEE Journal on Selected Areas in Communications*, vol. 36, no. 11, pp. 2486–2496, Nov. 2018.
- [6] G. Karabulut Kurt, M. G. Khoshkholgh, S. Alfattani, A. Ibrahim, T. S. J. Darwish, M. S. Alam, H. Yanikomeroglu, and A. Yongacoglu, "A vision and framework for the high altitude platform station (HAPS) networks of the future," *IEEE Communications Surveys Tutorials*, vol. 23, no. 2, pp. 729–779, Secondquarter 2021.
- [7] Q. Ren, O. Abbasi, G. K. Kurt, H. Yanikomeroglu, and J. Chen, "Caching and computation offloading in high altitude platform station (HAPS) assisted intelligent transportation systems," *arXiv preprint arXiv:2106.14928*, 2021.
- [8] J. Kokkonen, J. Lehtomäki, and M. Juntti, "A line-of-sight channel model for the 100–450 gigahertz frequency band," *EURASIP Journal on Wireless Communications and Networking*, vol. 2021, no. 1, pp. 1–15, Apr. 2021.
- [9] A. Al-Hourani, S. Kandeepan, and S. Lardner, "Optimal LAP altitude for maximum coverage," *IEEE Wireless Communications Letters*, vol. 3, no. 6, pp. 569–572, Dec. 2014.
- [10] V. Petrov, D. Moltchanov, and Y. Koucheryavy, "Interference and SINR in dense terahertz networks," in *2015 IEEE 82nd Vehicular Technology Conference (VTC-Fall)*, pp. 1–5.
- [11] A. Agrawal and S. Boyd, "Disciplined quasiconvex programming," *Optimization Letters*, vol. 14, no. 7, pp. 1643–1657, 2020.